Available online at www.sciencedirect.com
SCIENCE DIRECT®
ELSEVIER
ISPRS Journal of Photogrammetry & Remote Sensing 58 (2004) 315–329
PHOTOGRAMMETRY & REMOTE SENSING
www.elsevier.com/locate/isprsjprs

From point-based to feature-based aerial triangulation

T. Schenk *

The Ohio State University, CEEGS Department, 2070 Neil Ave., Columbus, OH 43210, USA

Received 6 December 2003; received in revised form 25 February 2004; accepted 27 February 2004
Available online 26 April 2004

Abstract

This paper is concerned with using linear features in aerial triangulation. Without loss of generality, the focus is on straight lines with the attempt to treat tie lines in the same fashion as tie points. The parameters of tie lines appear in the block adjustment like the tie points do. This requires a unique representation of lines in object space. We propose a four-parameter representation that also offers a meaningful stochastic interpretation of the line parameters. The proposed line representation lends itself to a parameterized form, allowing use of the collinearity model for expressing orientation and tie line parameters as a function of points measured on image lines. The paper describes in detail the derivation of the extended collinearity model and discusses the advantages of this new approach compared to the standard coplanarity model that is used in line photogrammetry. The intention of the paper is to make a contribution to feature-based aerial triangulation on the algorithmic level.

Keywords: aerial triangulation; line-photogrammetry; feature-based orientation; automation; linear features

1. Introduction

A major benefit of digital photogrammetry is its potential for automation. For example, automatic aerial triangulation sets out to perform all the necessary processes automatically, with as little help from a human operator as possible. Although remarkable progress has been achieved during the past few years, fully automatic aerial triangulation remains an elusive goal. The main obstacle is the block adjustment that is still point-based. In turn, this tends to force the processes of extracting and matching features also to be point-based. Now, point-based methods work extremely well in traditional photogrammetry where human operators make good use of their complex image understanding capacities to identify and measure points. The mental faculty of understanding images without conscious effort is still far beyond the capabilities of a machine, however. Hence, it is not a surprise that point-based photogrammetry has its limits in view of automation.

In the attempt of making processes more robust and thus suitable for automation, the computer vision community has long turned to feature-based methods. Over the years, several researchers in photogrammetry have also strongly argued for using features instead of points (Masry, 1981; Heikkilä, 1991; Kubik, 1992; Mikhail, 1993; Förstner, 2000; Schenk, 2002). The salient points brought forward are summarized as follows:

- human operators employ sophisticated image understanding processes and bring to bear photo-

* Tel.: +1-614-292-7126; fax: +1-614-292-2957.
E-mail address: schenk.2@osu.edu (T. Schenk).

0924-2716/$ - see front matter © 2004 Elsevier B.V. All rights reserved.
doi:10.1016/j.isprsjprs.2004.02.003

grammetric knowledge and experience when selecting points, resulting in a high point quality (location, accuracy) that may even include semantic information (corner of a building). In contrast, points extracted by computer operators are far inferior in quality (arbitrary location, no semantic information),

- a typical aerial scene contains more linear features than well-defined points,[1]
- control information from object space is more readily available in the form of features than points for the purpose of orienting imagery,
- establishing correspondences between features in different images and/or images and object space is more reliable than point matching,
- the automation chain of photogrammetric processes (e.g., orientation→surface reconstruction→object recognition) begins with features.

The idea of using features in photogrammetry is not new. Lugnani (1980) demonstrated the use of digital entities as control information, and at the ISPRS Congress 1988 two papers addressed the issue of linear features. Tommaselli and Lugnani (1988) concentrated on straight lines while Mulawa and Mikhail (1988) included also conic sections. These pioneering publications sparked great interest, particularly in architectural photogrammetry where straight-line features are abundant. Subsequently, line photogrammetry emerged as a new field. For an excellent overview of this subject, the reader is referred to Heuvel (2003, chapter 1). So far, line photogrammetry has not had a major impact on aerial triangulation, however. Whenever a feature-based approach is claimed in aerial triangulation, a closer look reveals that points are meant, because bundle block adjustment programs use tie points and not tie lines.

Common to the overwhelming approach of line photogrammetry is what we call the *coplanarity approach* in this paper. Here, a condition is formulated that forces the projection planes in the image and object space to become identical. This is in contrast to the *collinearity approach* where the projection rays are mathematically modeled to intersect the line in object space, and the projection plane in image space is neither used nor necessary. The projection plane, defined by the projection center and the line in image or object space is also called definition plane or interpretation plane in line photogrammetry. We use projection plane in this paper, and projection ray for the "bundle" ray from the perspective center through an image point to the line in object space.

This paper pursues the collinearity approach where the relationship between image feature and object space feature is modeled by the collinearity equations. This requires a parametric representation of the object space line. Moreover, the object space line must be uniquely represented by four parameters that also allow a meaningful stochastic interpretation. Analogously to tie points, straight lines in object space become *tie lines*. Like tie points, tie lines are directly modeled and appear as explicit parameters in the block adjustment.

The next section summarizes the use of linear features for orienting images. In addition, we discuss briefly the differences between the coplanarity and collinearity approaches. Section 3 discusses the requirements for an optimal geometric and stochastic line model. The proposed four-parameter representation is unique and lends itself to a parametric line representation, which is necessary for employing the collinearity model. Section 4 introduces tie lines into the block adjustment, explicitly expressed with their line parameters. This is accomplished by extending the collinearity equations to include the line parameters. The adjustment model estimates the orientation and the line parameters simultaneously. One of the advantages of the proposed collinearity approach is the flexible and transparent handling of control information, such as full and partial control lines, parallel lines, and parallel lines with a known distance between them.

To show the application and to demonstrate the feasibility of the proposed method, we describe in Section 5 a small example of a block adjustment with tie lines. The paper concludes with a brief summary and an outlook on new applications and future research.

The intent of this paper is to make a contribution towards feature-based aerial triangulation on the algorithmic level. The algorithms presented in Sections 3

[1] Usually, end points of linear features are not well defined. Although a linear feature may be distinct, its end points are not distinct points.

and 4 should allow for an implementation of a bundle block adjustment with straight lines. In the interest of brevity, other important issues, such as establishing correspondences of tie lines and control lines, and initial parameter estimation, are not addressed.

2. Background

2.1. Using features in aerial triangulation

Features occur in image and object space and include areal and linear entities. Linear features can be grouped into straight lines, conic sections, analytical curves, and free-form curves. Following a similar categorization for areal features, we may distinguish between planes, analytical surfaces, and free-form surfaces, such as DEMs. In *feature-based aerial triangulation*, all of these feature types may be used while *line photogrammetry* is usually restricted to the class of straight lines. The proposed method in this work lends itself to the use of conic sections and analytical space curves.

Initial efforts of line photogrammetry were directed towards the orientation of a single image with straight lines. A common characteristic of the proposed methods is the coplanarity approach that forces the image and object projection planes to become identical. Variations in the suggested methods consist of including the interior orientation, or of dealing with special cases, for example, the orientation with parallel lines (Heuvel, 2003). Another important aspect of line photogrammetry is the combination of orientation and the reconstruction of parameterized objects (object modeling).

Attempts at using linear features in aerial triangulation are almost exclusively restricted to the orientation of single images (single photo resectioning). Although the original publications by Mulawa and Mikhail (1988) and Tommaselli and Lugnani (1988) specifically mention the collinearity model and parameterized lines, subsequent work embraced the coplanarity model. Zalmanson (2000) was the first to rigorously pursue the use of parameterized linear control features for image orientation. The author successfully incorporated conic sections, 3D space curves, and—most importantly from a practical viewpoint—free form lines. Habib et al. (2002) propose the combination of matching (establishing correspondence between image and control line) with orientation with a modified Hough transformation, thus avoiding the classical adjustment method for parameter estimation. In Läbe and Henze (2002), the authors describe a procedure to orient single images fully automatically by using 3D building models as control information.

Orienting images is not restricted to linear control features. Ebner and Strunz (1988) suggested orienting stereomodels with respect to DEMs using a target function that minimizes the z-differences. Jaw (1999) successfully demonstrated how control surfaces can be used in aerial triangulation by extending the independent model method to include a relationship between model point and planar surface patch, with a target function that minimizes the distances along the surface normal.

2.2. Mathematical models for incorporating linear features

There are two principally different ways to establish a relationship between image and control features. In the first approach, the image feature is represented as an entity like the control feature. This entails fitting a straight line or a curve through instances of the image feature. Then, a relationship between image and object space lines are formed by forcing the projection planes to become identical, referred to here as the *coplanarity model*.

The second approach takes a point of the image feature, for example an edge pixel, and forces the projection ray to intersect the control line by minimizing the residuals of the observed image point. In this paper, this point-to-line approach is appropriately called the *collinearity model*.

2.2.1. Coplanarity approach

The basic idea of the coplanarity approach is to formulate a constraint such that the projection planes in image space and object space become identical (coplanar). Such a constraint can be formulated as

$$\lambda \mathbf{R}\mathbf{n}' = \mathbf{n} \tag{1}$$

with λ a scale factor, $\mathbf{R}$ the attitude matrix, $\mathbf{n}'$ the normal of the plane defined by the perspective center

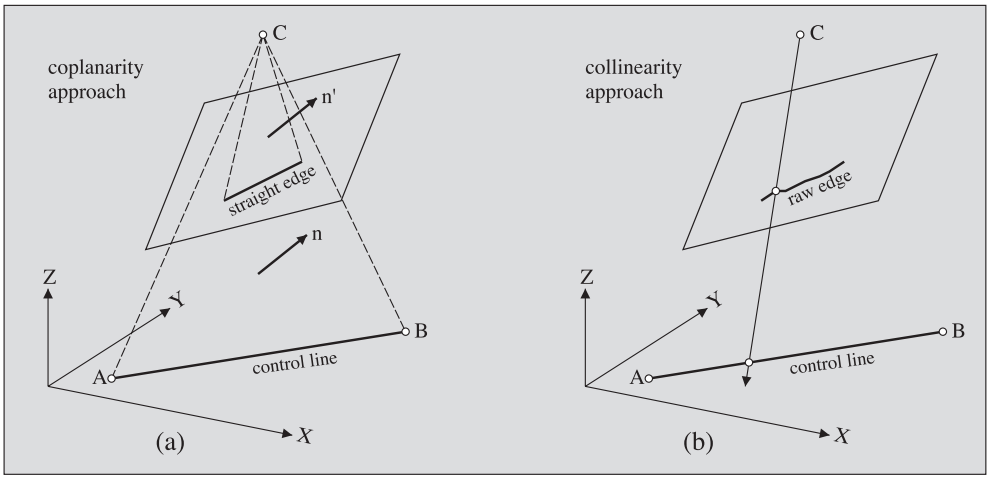

Fig. 1. Illustration of coplanarity (a) and collinearity approach (b) to establish relationships between object space lines and their partial projections in images.

C and image line L', and **n** the normal of the plane defined by the perspective center C and control line L. Fig. 1a illustrates the concept. Over the years, several variations of this basic formulation have been suggested (e.g., Tommaselli and Lugnani, 1988; Mulawa and Mikhail, 1988; Patias et al., 1995; Habib, 1999; Heuvel, 2003).

2.2.2. Collinearity approach

Suppose a known straight line in object space (control line) is partially imaged and detected by an edge operator, for example. We can extend the standard collinearity model such that the projection ray from the perspective center through an edge point intersects the control line. Fig. 1b illustrates this scenario. The parametric representation of the control line conveniently describes this circumstance. Let the line be represented by point $A=(X_A, Y_A, Z_A)$ and direction vector $\mathbf{d}=(a, b, c)$. Then any point on the line is defined by

$$X = X_A + t \cdot a$$

$$Y = Y_A + t \cdot b$$

$$Z = Z_A + t \cdot c \qquad (2)$$

with t a real variable denoted as the line parameter. Now, in the standard collinearity model we substitute object point P by the above expression to obtain the extended model

$$x_p = -f\frac{(X_A + t\cdot a - X_C)r_{11} + (Y_A + t\cdot b - Y_C)r_{12} + (Z_A + t\cdot c - Z_C)r_{13}}{(X_A + t\cdot a - X_C)r_{31} + (Y_A + t\cdot b - Y_C)r_{32} + (Z_A + t\cdot c - Z_C)r_{33}}$$

$$y_p = -f\frac{(X_A + t\cdot a - X_C)r_{21} + (Y_A + t\cdot b - Y_C)r_{22} + (Z_A + t\cdot c - Z_C)r_{23}}{(X_A + t\cdot a - X_C)r_{31} + (Y_A + t\cdot b - Y_C)r_{32} + (Z_A + t\cdot c - Z_C)r_{33}} \qquad (3)$$

with x_p, y_p an observed edge point, f the focal length, r_{ij} the elements of the orthogonal rotation matrix, and X_C, Y_C, Z_C the coordinates of the perspective center. In addition to the six exterior orientation parameters, we have also the line parameters t as unknowns to be estimated. Considering the degrees of freedom of two for straight 2D lines, another independent observation equation of the form 3 can be formed. Not surprisingly, three non-collinear control lines[2] are needed to determine the exterior orientation parameters. Observing more than two points on an image line does not reduce the rank deficiency but increases the redundancy and thus positively influences the accuracy. Note that even if only one point per line is used, the orientation can be solved. However, we would need six control lines in that case.

[2] 3×4 equations, six orientation unknowns, six unknown line parameters.

2.2.3. Discussion of the two approaches

The coplanarity approach is intuitively simple. Nevertheless, it has several disadvantages. For one, it restricts the shape of features to straight lines. In contrast, the collinearity model can easily be extended to higher-order features, for example, conic sections, polynomials, or any 3D curve that allows a parametric representation. For an extensive discussion of this subject, the reader is referred to Zalmanson (2000).

Another major difference between the two methods lies in the representation of the feature in image space. The coplanarity model requires a straight image line while the collinearity model works with any point of the image line, for example, edge pixels. Usually, it is not possible to determine straight lines in images directly. Rather, straight lines are obtained by a sequence of processes, such as detecting, linking, and segmenting edges. The collinearity model can work with lower level primitives (e.g., edge pixels), which may be advantageous at times. On the other hand, it also copes with straight lines by taking their end points. Using all pixels of the image line or only the two endpoints of the fitted line lead to identical results if the covariance matrix of the line fitting process is used as the weight for the two end points. In this way, the collinearity model can be seen as combining the line fitting process with the subsequent orientation and/or reconstruction task.

3. Line representation

Linear features are very prominent descriptors of our physical world. Boundaries of man-made objects can often be abstracted by straight lines. A straight line is a fundamental primitive of feature-based photogrammetry. In view of solving photogrammetric problems, such as orientation and reconstruction, it is important to have a good representation for a line. This section summarizes desirable requirements for a good representation, examines existing representations, and presents an optimal solution.

3.1. Requirements for optimal representation

To effectively solve the fundamental tasks of orientation and reconstruction with straight lines, an optimal line representation in Euclidean 3D space should meet the following requirements:

- number of parameters should be equal to the degrees of freedom of a 3D line,
- the representation should be unique and free of singularities,
- there should be a one-to-one correspondence between the representation and the definition of the line, e.g., by one point and the direction,
- the four parameters should allow a meaningful stochastic interpretation,
- the representation should be suitable for parametric expression.

A straight line in 3D space has four independent degrees of freedom. Let $\mathscr{L}$ be a line defined by point $\mathbf{p}=(X_p, Y_p, Z_p)$ and direction vector $\mathbf{d}=(a, b, c)$, referred to as *point-orientation definition*, $\mathscr{L}(\mathbf{p}, \mathbf{d})$. Let the same line be represented in the four independent parameters (e, f, g, h), for example. Then, a one-to-one correspondence exists if the set of lines $\mathscr{L}\{\mathbf{p}, \mathbf{d}\}$ uniquely maps into a set of lines $\mathscr{L}\{e, f, g, h\}$ and vice versa, without the need for conditional interpretations or handling special cases.

Another important criterion is a meaningful and plausible interpretation of the stochastic properties of the line representation. For example, it should be possible to derive from the covariance matrix error quantities that only reflect the geometry of the line determination. Lines of the same precision should have the same error estimates, regardless of their position and orientation in the 3D coordinate frame.

3.2. Typical representations used in photogrammetry

The standard representation used in photogrammetry is the point-orientation definition, $\mathscr{L}(\mathbf{p}, \mathbf{d})$. This is not a unique solution because there are an infinite number of points that can be chosen, and many ways to represent the direction. To make it unique, two constraints are added, one related to the selection of the point (e.g., nearest point to origin, expressed by $\mathbf{p}\cdot\mathbf{d}=0$). The second constraint resolves the direction and sign ambiguity. Compared with a four-parameter representation, the point-orientation form with six parameters and two constraints is unnecessarily complicated. Moreover, the stochastic

interpretation is not unique as it depends on the choice of **p**.

Four-parameter representations have also been proposed. Zielinski (1993) uses three angles and a distance. The polar coordinates of a point on a 3D line closest to the origin determine three parameters. The third angle is defined in the plane that is perpendicular to the direction from the origin to the closest point. Obviously, this four-parameter representation degenerates for lines passing through the origin or intersecting with the Z-axis. Other four-parameter representations are based on the intersection of two planes. Ayache and Faugeras (1989) suggested using one plane parallel to the x-axis and the other plane parallel to the y-axis. This representation is flawed by singularities for it cannot represent lines that are perpendicular to the z-axis. In addition, the stochastic properties of this representation are not transparent.

3.3. Optimal representation

Following Roberts (1988), the proposed representation of a line is based on two orientation parameters and two positional parameters. The two orientation parameters obviously express the direction of the line. To envision the two positional parameters, imagine a plane perpendicular to the line and passing through the origin of the coordinate system. The line intersects this plane at a point whose position forms the remaining two parameters. Note that this point is the closest point to the origin.

Let $\mathscr{L}$ be a line given in a 3D Cartesian coordinate frame O-XYZ. Let O-$X'Y'Z'$ be a coordinate frame with the same origin but rotated such that its Z'-axis becomes parallel to $\mathscr{L}$. The rotation between the two coordinate frames is defined by the two angles that specify the line direction. The third angle, namely, the rotation about the line itself, is irrelevant and can be fixed, for example, by setting it to zero.

A suitable selection of two independent angles is the conversion of Cartesian coordinates to spherical coordinates. Let ϕ denote the azimuth (longitude) and θ the zenith (90° minus latitude). These two angles, bounded by $0 \le \phi \le 2\pi$ and $0 \le \theta \le \pi$, uniquely define all possible directions of line $\mathscr{L}$. Note that for vertical lines to the X,Y-plane, the undefined azimuth is set to zero.

Line $\mathscr{L}$ intersects the X' Y' plane. Let (x_o, y_o) be the coordinates of this intersection in the O-$X'Y'Z'$ system. Then, the 4-tuple (ϕ, θ, x_o, y_o) is the four-parameter representation. Fig. 2 illustrates the concept. This representation, denoted by $\mathscr{L}\{\phi, \theta, x_o, y_o\}$, is simple, aesthetically pleasing, and has a unique one-to-one mapping. Moreover, it gives equal importance to angles and positions—an advantage that is particularly evident in performing elementary transformations with the line, and in the stochastic interpretation of the line parameters.

3.3.1. Mapping between point-orientation and four-parameter representation

Given is a line $\mathscr{L}$ in its point-orientation form $\mathscr{L}\{\mathbf{p}, \mathbf{d}\}$ as defined above. To find the line's four-

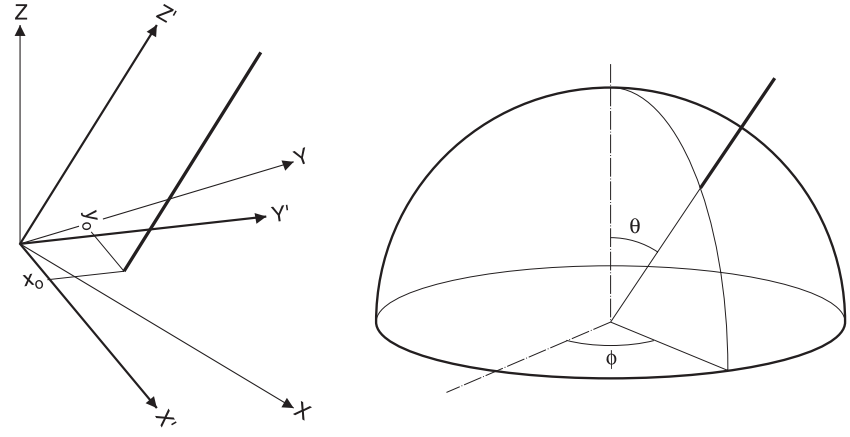

Fig. 2. Illustration of the concept of the four-parameter representation. Two parameters define the direction of line $\mathscr{L}$, and its intersection with a plane perpendicular to it defines the two positional parameters. The line is uniquely represented by the 4-tuple (ϕ, θ, x_0, y_0).

parameter representation, we proceed as follows. The direction vector **d** is converted to spherical coordinates ϕ, θ, ρ, with ϕ the azimuth, θ the zenith angle, and ρ the radius of the sphere. The radius is not needed, hence **d** does not need to be a unity vector. With the two angles we form rotation matrix $\mathbf{R}_{\phi\theta}$

$$\mathbf{R}_{\phi\theta} = \begin{bmatrix} \cos\theta\cos\phi & \cos\theta\sin\phi & -\sin\theta \\ -\sin\phi & \cos\phi & 0 \\ \sin\theta\cos\phi & \sin\theta\sin\phi & \cos\theta \end{bmatrix} \tag{4}$$

$\mathbf{R}_{\phi\theta}$ rotates point **p** of the point-orientation form into the new coordinate system whose z-axis is parallel to the straight line. Then the rotated point vector $\mathbf{p}'$ is expressed by:

$$\mathbf{p}' = \mathbf{R}_{\phi\theta}\mathbf{p} = \begin{bmatrix} x_o \\ y_o \\ z \end{bmatrix} \tag{5}$$

In fact, any point $\mathbf{p}_i=(X_i, Y_i, Z_i)$ on the line will render the same planimetric coordinates (x_o, y_o) but a different z-coordinate. We realize that z_i can be viewed as the parameter in the parametric form of the line representation. Hence, the parametric form of the line representation is symbolically denoted by $\mathscr{L}\{\phi, \theta, x_o, y_o, z\}$.

The inverse relationship of Eq. (5) maps any point in the four-parameter representation to a unique point in the original point-orientation form of line $\mathscr{L}$:

$$\mathbf{p} = \mathbf{R}_{\phi\theta}^{T}\mathbf{p}' = \begin{bmatrix} X \\ Y \\ Z \end{bmatrix} = \begin{bmatrix} \cos\theta\cos\phi \cdot x_o - \sin\phi \cdot y_o + \sin\theta\cos\phi \cdot z \\ \cos\theta\sin\phi \cdot x_o + \cos\phi \cdot y_o + \sin\theta\sin\phi \cdot z \\ -\sin\theta \cdot x_o + \cos\theta \cdot z \end{bmatrix} \tag{6}$$

3.3.2. Stochastic interpretation of proposed representation

Suppose a straight line is measured on $n>2$ images. Let us for a moment assume that the orientation of the images is known, including their standard deviations. Let us further assume that the measurements also have random errors. Employing an adjustment procedure will yield estimates of the four line parameters. Moreover, the covariance matrix will contain information for a statistical analysis. Can we derive error properties for a line in order to judge if the results are satisfactory?

Here follows a geometric interpretation. The errors on ϕ and θ can be conceived as a cone whose axis is identical to the direction of the line. Since the two angles are spherical coordinates, one can imagine an error figure on the sphere. The error figure is centered at ϕ, θ. The line "wiggles" within this error figure, but the center is fixed. Fig. 3 depicts a graphical interpretation of these errors.

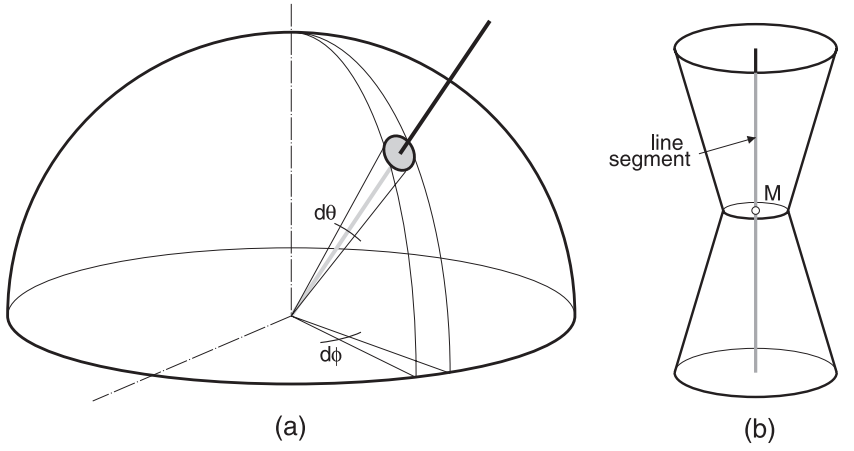

Fig. 3. Illustration of random errors of a line segment. The errors on the two angles ϕ, θ describe a cone, shown in (a). The errors on the midpoint of the line segment, obtained by error propagation, can be conceived as an error ellipse. The combination of these error sources is depicted in (b).

The errors on the location parameters x_o, y_o are described by an error ellipse. Unfortunately, they depend on the coordinate system. However, we never have infinitely long straight lines in reality. For example, lines that represent object boundaries are of finite length. Thus, it makes sense to consider line segments. In turn, this suggests determining the errors of the midpoint M of the line segment. This is readily accomplished by way of error propagation, using the 4×4 covariance of the adjusted line and Eq. (6) that expresses M as a function of the estimated line parameters. Then, the combination of these errors would lead to a cone that is moved around the error ellipse derived for mid-point M (see Fig. 3).

Normally, the 4×4 covariance matrix of a tie line is obtained from the block adjustment. An interesting situation arises if the stochastic properties are to be derived from a priori information about a straight line. Such is the case for known lines that may enter the adjustment as control lines. We derive the covariance matrix of control lines from two known points and their covariances in Section 4.2.2.1.

Obviously, this geometric interpretation of the errors of the line parameters gives only an approximate description of the errors. A more correct error figure would be obtained by determining the variance covariance matrices for many points on the line. For more details, the interested reader is referred to Schenk (2004, chapter 19).

4. Block adjustment with lines

In the previous section, we have laid the foundation for using straight lines in aerial triangulation. Following the discussion of the coplanarity vs. collinearity approach, we favor the latter because it is more general and simpler to implement. We first derive an extended collinearity model capable of handling control and tie lines and sketch the adjustment model.

4.1. Extended collinearity equations

To accommodate linear features in the collinearity model, it is of paramount importance to represent the feature in parametric form. Parametric representations of features in object space allow the specification of any point on the feature. In the case of the collinearity model, we are seeking the closest point on the feature to the projection ray.

Recall that Eq. (6) defines a parametric representation of 3D straight lines. It expresses the relationship between an arbitrary point **p** on the 3D line and the four-parameter representation. We give this equation again since it is the starting point for deriving the extended collinearity equations.

$$\begin{bmatrix} X \\ Y \\ Z \end{bmatrix} = \begin{bmatrix} \cos\theta\cos\phi \cdot x_o - \sin\phi \cdot y_o + \sin\theta\cos\phi \cdot z \\ \cos\theta\sin\phi \cdot x_o + \cos\phi \cdot y_o + \sin\theta\sin\phi \cdot z \\ -\sin\theta \cdot x_o + \cos\theta \cdot z \end{bmatrix} \tag{7}$$

Eq. (7) explicitly describes the coordinates (X, Y, Z) of an arbitrary point on the straight line as a function of the four parameters (ϕ, θ, x_o, y_o) of the line, which is parameterized in the real variable z.

Let

$$x = -c\frac{u}{w} \quad y = -c\frac{v}{w} \tag{8}$$

denote the standard collinearity equations for points with x, y the refined[3] photo coordinates, c the calibrated focal length, and with

$$\begin{aligned} u &= (X - X_C)r_{11} + (Y - Y_C)r_{12} + (Z - Z_C)r_{13} \\ v &= (X - X_C)r_{21} + (Y - Y_C)r_{22} + (Z - Z_C)r_{23} \\ w &= (X - X_C)r_{31} + (Y - Y_C)r_{32} + (Z - Z_C)r_{33} \end{aligned} \tag{9}$$

Substituting (X, Y, Z) in Eq. (9) by the expressions found in Eq. (7) leads to

$$\begin{aligned} u &= (\cos\theta\cos\phi \cdot x_o - \sin\phi \cdot y_o + \sin\theta\cos\phi \cdot z - X_C)r_{11} + (\cos\theta\sin\phi \cdot x_o + \cos\phi \cdot y_o + \sin\theta\sin\phi \cdot z - Y_C)r_{12} + (-\sin\theta \cdot x_o + \cos\theta \cdot z - Z_C)r_{13} \\ v &= (\cos\theta\cos\phi \cdot x_o - \sin\phi \cdot y_o + \sin\theta\cos\phi \cdot z - X_C)r_{21} + (\cos\theta\sin\phi \cdot x_o + \cos\phi \cdot y_o + \sin\theta\sin\phi \cdot z - Y_C)r_{22} + (-\sin\theta \cdot x_o + \cos\theta \cdot z - Z_C)r_{23} \\ w &= (\cos\theta\cos\phi \cdot x_o - \sin\phi \cdot y_o + \sin\theta\cos\phi \cdot z - X_C)r_{31} + (\cos\theta\sin\phi \cdot x_o + \cos\phi \cdot y_o + \sin\theta\sin\phi \cdot z - Y_C)r_{32} + (-\sin\theta \cdot x_o + \cos\theta \cdot z - Z_C)r_{33} \end{aligned} \tag{10}$$

Entering u, v, w of Eq. (10) in Eq. (8) leads to the modified collinearity equations. They contain the four line parameters ϕ, θ, x_o, y_o, parameter z,

[3] Photo coordinates reduced to principal point, corrected for radial distortion and atmospheric refraction.

and the exterior orientation parameters (perspective center X_C, Y_C, Z_C and attitude matrix with the elements $r_{11}, \ldots, r_{33}$).

4.2. Adjustment model

The extended collinearity equations for straight lines express observations (point coordinates of measured features) as a nonlinear function of orientation parameters and line parameters. After linearization of Eq. (10) with respect to the parameters, we can employ the Gauss–Markov model for estimating the unknowns.

$$\mathbf{y} = \mathbf{A}\xi + \mathbf{e}, \qquad \mathbf{e} \sim (0, \sigma_o^2 \mathbf{P}^{-1}) \tag{11}$$

with $\mathbf{y}$ the observation vector, $\mathbf{A}$ the design matrix, ξ the parameters to be estimated, and with $\mathbf{e}$ the error vector. The parameters are estimated such that the collinearity equations are satisfied by minimizing the square sum of the residuals of the points measured on image lines.

Let us arrange the parameters into three groups: ξ_E contains the exterior orientation parameters, ξ_L the line parameters, and ξ_Z the point parameters. We also add control information to remove the rank deficiency associated with the normal equation system obtained from Eq. (11). Control information may enter the adjustment model through stochastic constraints on either ξ_E (e.g., in direct orientation) or ξ_L (e.g., control lines).

Eq. (11) is now partitioned as follows

$$\begin{bmatrix} \mathbf{y}_E \\ \mathbf{y}_L \\ \mathbf{y}_Z \end{bmatrix} = \begin{bmatrix} \mathbf{A}_E & \mathbf{A}_L & \mathbf{A}_Z \\ 0 & \mathbf{A}_L^C & 0 \\ \mathbf{A}_E^C & 0 & 0 \end{bmatrix} \begin{bmatrix} \xi_E \\ \xi_L \\ \xi_Z \end{bmatrix} + \begin{bmatrix} \mathbf{e}_E \\ \mathbf{e}_L \\ \mathbf{e}_Z \end{bmatrix} \tag{12}$$

where

- $\mathbf{A}_E$ is a $2{\cdot}p \times 6{\cdot}n$ matrix containing the partial derivatives of the extended collinearity equations with respect to the exterior orientation parameters while ξ_E contains the changes to the parameters,
- $\mathbf{A}_L$ is a $2{\cdot}p \times 4{\cdot}m$ matrix containing the partial derivatives of the extended collinearity equations with respect to the line parameters while ξ_L contains the changes to the parameters,
- $\mathbf{A}_Z$ is a $2{\cdot}p \times p$ matrix containing the partial derivatives of the extended collinearity equations with respect to parameter Z while ξ_Z contains the changes to the parameters,
- $\mathbf{A}_E^C$ is a $r \times 6{\cdot}r$ matrix containing the stochastic constraints on the exterior orientation parameters,
- $\mathbf{A}_L^C$ is a $s \times 4{\cdot}s$ matrix containing the stochastic constraints on the line parameters (control lines)

and with n number of images in block adjustment; m number of lines in block adjustment; p total number of measured points on image lines; r number of stochastic constraints on exterior orientation parameters; s number of stochastic constraints on line parameters (control lines).

With the notation of Eq. (12), the following normal equations are obtained:

$$\begin{bmatrix} \mathbf{N}_{EE} + \mathbf{N}_{EE}^C & \mathbf{N}_{EL} & \mathbf{N}_{EZ} \\ \mathbf{N}_{EL}^T & \mathbf{N}_{LL} + \mathbf{N}_{LL}^C & \mathbf{N}_{LZ} \\ \mathbf{N}_{EZ}^T & \mathbf{N}_{LZ}^T & \mathbf{N}_{ZZ} \end{bmatrix} \begin{bmatrix} \hat{\xi}_E \\ \hat{\xi}_L \\ \hat{\xi}_Z \end{bmatrix} = \begin{bmatrix} \mathbf{c}_E \\ \mathbf{c}_L \\ \mathbf{c}_Z \end{bmatrix} \tag{13}$$

$\mathbf{N}_{EE}$ and $\mathbf{N}_{LL}$ are diagonal matrices with 6×6 and 4×4 submatrices, respectively. $\mathbf{N}_{ZZ}$ is purely diagonal with $2\times p$ elements. This special structure allows algebraic elimination of one of the parameter vectors. Considering the size, it is suggested to eliminate ξ_Z. Note that $\mathbf{N}_{EE}^C$ and $\mathbf{N}_{LL}^C$ contain the contributions from control information brought into the system by stochastic constraints (pseudo observations) on the orientation parameters and line parameters.

4.2.1. Redundancy considerations

Let us briefly discuss the redundancy budget. Every tie line has four parameters and every point measured on a tie line adds one additional parameter (z-parameter). Let n be the number of points measured on an image line and m the number of images in which the tie line is measured. Then we have $2{\cdot}n{\cdot}m$ equations and $4+n{\cdot}m$ unknowns, resulting in a redundancy of $r=n{\cdot}m-4$. Since the degrees of freedom of a 2D line are four, only two points per image line are independent, that is $r=2{\cdot}m-4$. Measuring a tie line on two images ($m=2$) is just enough to determine the four

line parameters—no redundant information is available towards the computation of the orientation parameters. This confirms that the orientation of two images (relative orientation) with straight lines is not possible, except when using epipolar lines. To conclude, a tie line must appear on at least three images to make a contribution towards the orientation parameters—in other words, to tie the images together. We call this contribution the *information content*, *ic*, of a tie line, rather than redundancy.

Suppose now that there are t tie lines per image. Then the information content will be $ic=t(2\cdot m-4)$ for t tie lines that appear on m images. Considering that every image has six exterior orientation parameters, we can easily determine how many tie lines are needed to completely orient the images. Take the case of an image triple, for example. Its relative orientation involves $3\times6-7=11$ unknowns. Hence, six tie lines suffice to orient the triplet, because the *information content* will be $ic=6(2\cdot3-4)=12$.

Tie points contribute $r=2\cdot m-3$ to the redundancy budget, that is, one more independent equation compared to tie lines. There is a huge difference between tie lines and tie points, however. Tie points must be identified (matched) on all images involved while points on tie lines can be measured monocularly. Moreover, tie lines are not restricted to the physical overlap of images, for they can be measured on all images with a partial projection of the tie line.

4.2.2. Control information

Control information refers to object space knowledge about lines and their relationships, or to information about the exterior orientation parameters (e.g., in case of direct orientation). This knowledge is usually explicitly available prior to aerial triangulation. It is also conceivable to apply general knowledge, for example, that lines with a certain orientation and distance between them should be parallel (e.g., railway tracks, vertical building edges). In this case, parallelism could be enforced after incidences of the general knowledge are found in the actual data set after a first adjustment.

Control information about lines enters the adjustment model through stochastic constraints on the line parameters ξ_L. Therefore, control lines must be represented in the same four-parameter representation as tie lines. Control information may be available for all four parameters, referred to as *full control line*, or only for the direction of the line, appropriately called *partial control line*.

4.2.2.1. Full control lines. Suppose a full control line is defined by the two known points A and B. Then the problem is to convert the two-point representation to the desired four-parameter representation. After determining the direction vector from A and B, parameters ϕ, θ are readily obtained by converting the direction vector to spherical coordinates. Eq. (5) computes the two remaining parameters. Control line $\mathscr{L}_c$ is now represented by the 4-tuple (ϕ, θ, x_o, y_o).

In order to express uncertainties of $\mathscr{L}_c$, the following procedure is suggested. Let σ_A and σ_B be the variances of the two points A and B that define $\mathscr{L}_c$. Let M be the mid-point of line segment A, B. Eq. (7) expresses the coordinates of an arbitrary point on the line as a function of the four parameters ϕ, θ, x_o, y_o and the line parameter z. This can be conceived as a Gauss–Markov model where the two endpoints A and B of the control line yield six equations with four unknown line parameters and the two unknown z_A, z_B parameters. After forming the normal equations, z_A, z_B can be eliminated and the inverse of this system is the covariance matrix of the line parameters.

4.2.2.2. Partial control lines. It is quite conceivable that for certain straight lines only the orientation is known. Examples include vertical lines, such as edges of buildings, or horizontal lines, either with known or unknown orientation (azimuth) in the X,Y-plane of the object space reference frame. The stochastic constraints for partial control lines are:

$$\text{vertical lines:}\quad \xi_\phi = 0 + e_\phi, \quad \xi_\theta = 0 + e_\theta \tag{14}$$

$$\text{oriented horizontal lines:}\quad \xi_\phi = \text{azimuth} + e_\phi, \quad \xi_\theta = \pi/2 + e_\theta \tag{15}$$

$$\text{horizontal lines:}\quad \xi_\theta = \pi/2 + e_\theta \tag{16}$$

4.2.2.3. Parallel lines. Other useful object space knowledge are parallel lines. Here, the position and the orientation are unknown, but the knowledge that

two tie lines are parallel can be considered with the following stochastic constraints:

$$\xi_{\phi_i} - \xi_{\phi_j} = 0 + e_{\phi_i} + e_{\phi_j}, \quad \xi_{\theta_i} - \xi_{\theta_j} = 0 + e_{\theta_i} + e_{\theta_j} \tag{17}$$

If the distance between the two parallel lines is known, then this can also be easily formulated as a stochastic constraint, in addition to Eq. (17). As these examples demonstrate, the proposed four-parameter representation of 3D lines lends itself to simple formulations for entering complex object space knowledge.

5. Experimental results

A small block with six images, 60% overlap and 30% strip overlap, serves as an example to demonstrate the feasibility of the proposed feature-based aerial triangulation method. The large-scale images, scale approximately 1:3800, cover part of the OSU campus with many man-made objects. The aerial film was scanned with 15 μm pixelsize, but for the experiments, this size was doubled. Hence, one pixel corresponds to approximately 0.11 m on the ground. Fig. 4 provides an overview and also depicts the tie lines that have been used in the block adjustment instead of tie points.

A Canny edge operator with a length specification of minimum 200 pixels was used to determine raw edges. Fig. 5 depicts the image patches of the 6-overlap area with the raw edges superimposed. From all these edges, we manually selected a few tie lines and established the correspondences between the different images. Since tie lines should appear on more than two images to contribute toward the orientation of images, we have only selected tie lines in the 3-overlap areas of strips, and in the 4-overlap and 6-overlap areas between strips. Fig. 4 shows the selected tie lines in these areas and Table 1 lists the number of tie lines and number of independent equations.

We briefly comment on the five tie lines in the 6-overlap area. They are annotated in both Figs. 4 and 5.

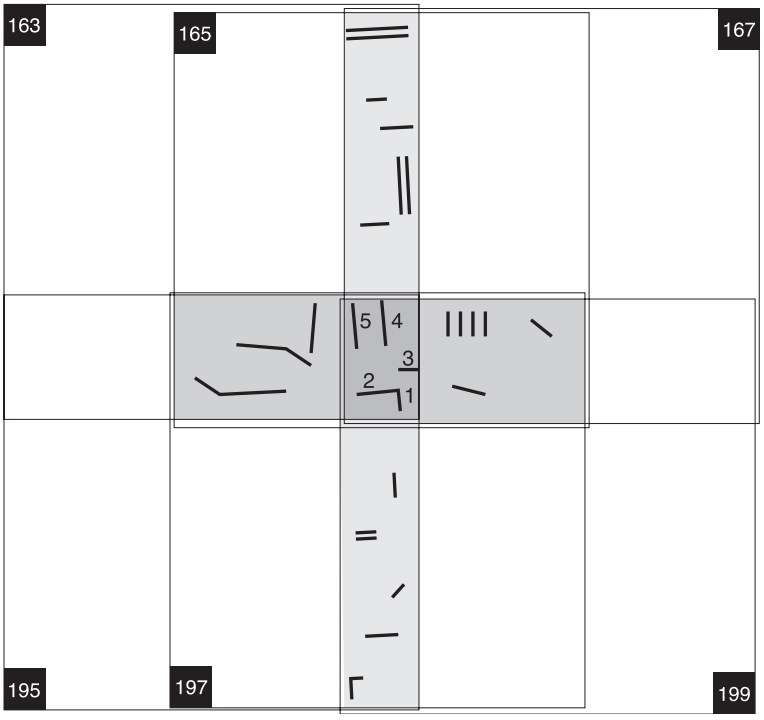

Fig. 4. Block configuration with six images and the tie lines used for the block adjustment. Only tie lines in the three, four, and six-overlap areas are used. The image patches covering the six-overlap area are shown together with extracted edges in Fig. 5.

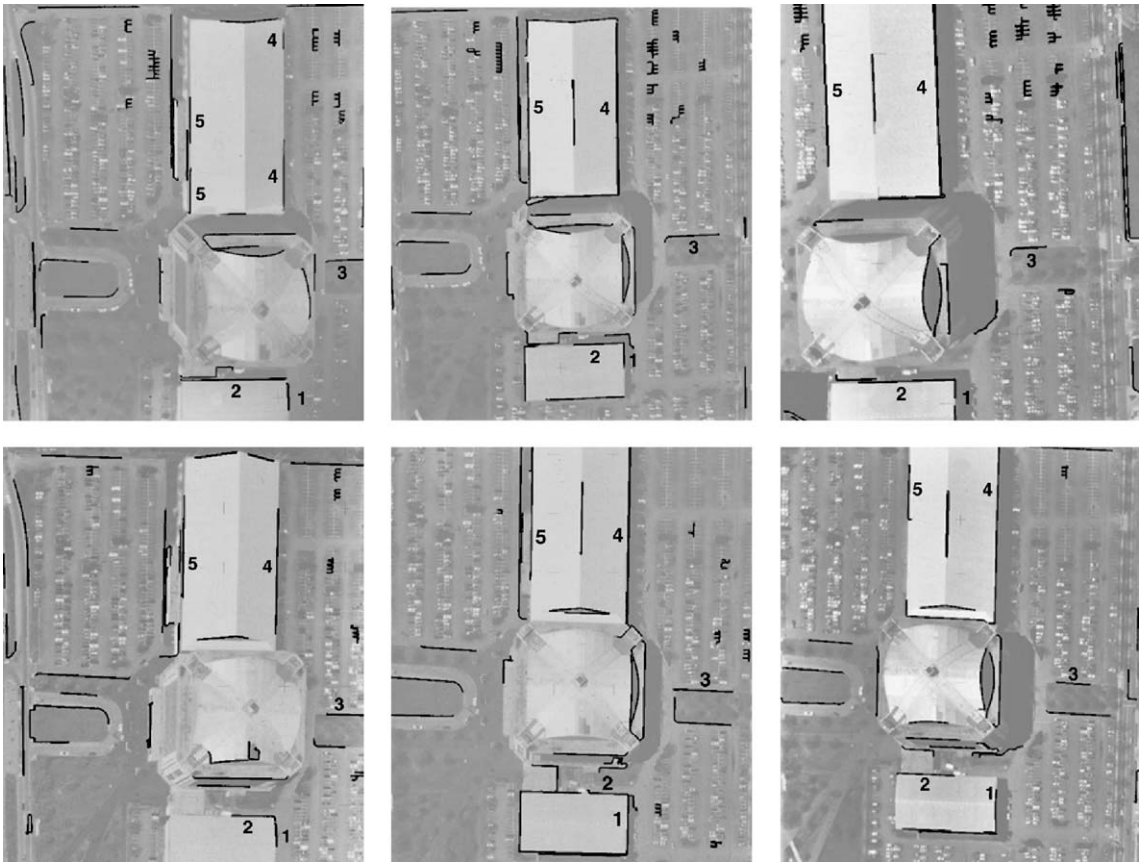

Fig. 5. The six image patches show the area covered by six photographs. Superimposed are the edges as obtained with the Canny operator. Five edges that appear on all six images are manually selected as tie lines. These selected tie lines are numbered 1 to 5 and also shown in Fig. 4.

Tie line 2 is a slanted roof edge of a building with a saddle roof. Tie line 1 is the horizontal continuation of the roof edge of the same building. Tie line 3 is the border of walkway. Tie lines 4 and 5 are again horizontal roof edges. Table 2 contains the length of the edges in the six images and also the total length of the tie line in object space, but expressed in image pixels. To convert the length into metric units, multiply the numbers by 0.11 m. As shown in detail in Schenk (2004, chapter 19), the ratio of the length of a tie line in an image and the total length of the tie line segment is a major factor that determines the accuracy

Table 1
Tie lines in the three, four, and six-overlap areas

Overlap area	Number of tie lines	Independent equations
3	14	168
4	11	176
6	5	120
Total	30	464

Table 2
Tie lines in the six-overlap area

Tie line	Total length	Edge length in images [pixels]					
		163	165	167	195	197	199
1	152	98	140	139	148	152	88
2	752	572	360	432	220	488	312
3	352	200	292	136	212	292	188
4	972	588	964	972	714	972	972
5	972	480	744	748	581	760	304

The second column contains the length of the tie line in object space but expressed in pixels. The length of each tie line in the six images is listed in columns 3–8. Among other factors, the length of the image lines determines the accuracy of the adjusted tie lines (see text for more details).

of a tie line. For example, image 199 contributes least to tie line 5 as the ratio is only 0.31.

We have approximated the raw edges of the tie lines by straight lines and used their endpoints for the collinearity equations (Eq. (10)). The weight was obtained from the line fitting process. The example block involves a total number of 30 tie lines. Column 3 of Table 1 lists the number of equations resulting from the 30 tie lines that are partially imaged in 3, 4, or 6 images. The total number of unknowns is $u=6\times6+30\times4+116\times2=388$. Thus, our sample block has a redundancy of $r=464-388=76$.

Since the sample block is very small, we have used a free block adjustment by fixing the six exterior orientation parameters of image 165 and the scale. The normalized normal equation system has a relatively low condition number ($\kappa=1.2\times10^3$) which indicates that the geometry of this mini block is good. The block adjustment also determines the four parameters of the tie lines as well as the z-parameter for every measured point. As an example of the precision of a (monocularly) measured point on a tie line, we give the variance covariance matrix of one of the endpoints of tie line 4, measured in image 165.

$$\begin{bmatrix} 3.25085e+006 & -1.62543e+007 & -3.58657e+006 \\ -1.62543e+007 & 8.12713e+007 & 1.79328e+007 \\ -3.58657e+006 & 1.79328e+007 & 1.44367e+007 \end{bmatrix}$$

This matrix was obtained by error propagation, using Eq. (7) to build the partial derivatives with respect to the parameters θ, ϕ, x_o, y_o, z of line 4. This matrix determines the variances and covariances among the three point coordinates. For example, the standard deviation of X would amount to $10^{-5}\times\sqrt{(3.25085e+006)}\approx0.02$ m, where 10 μm is the variance component. As one would expect from the orientation of tie line 4 (nearly parallel to the Y-axis of the object space coordinate system), the standard deviation ≈0.09 m for Y is considerably larger.

Future experiments will be concerned with establishing ground truth of tie lines to provide a realistic measure of the accuracy of tie lines in object space.

6. Summary and concluding remarks

The motivation for the research reported here is the attempt to treat tie lines in the same fashion as tie points. That is, the tie line parameters appear explicitly in the adjustment, just as the coordinates of tie points do. This requires a unique representation for 3D lines. Section 3 introduced a four-parameter representation that lends itself to a parameterized form and to a meaningful stochastic interpretation of the four line parameters. In particular, for every measured point on a tie line, the variance covariance matrices can be computed, leading to a point-wise, discrete error characterization of tie lines.

In comparing feature-based with point-based aerial triangulation we note these distinct differences:

- Feature-based aerial triangulation does not require conjugate points. Thus, it circumvents the thorny issue of matching points in multiple images. Instead, a more robust feature-matching scheme can be employed.
- In feature-based aerial triangulation, the overlap conditions of images are relaxed. In fact, tie lines can "tie" images together that do not overlap at all.
- Feature-based aerial triangulation offers more flexibility in incorporating object space knowledge. This is a distinct advantage when considering existing GIS with known information about straight lines.
- Feature-based aerial triangulation offers a greater potential for automation than point-based methods.

The proposed collinearity approach compares favorably with the coplanarity method, the preferred method in line photogrammetry. Specific advantages include:

- The collinearity approach can be extended to curves, such as conic sections and 3D space curves. In contrast, the coplanarity approach is limited to straight lines.
- The tie lines are uniquely represented by four parameters which enter the adjustment directly as unknowns. The coplanarity approach usually employs a six-parameter model with two constraints for an unambiguous representation. This

seems unnecessarily complicated, also in view of the stochastic interpretation of adjusted lines.
- The proposed approach handles object space knowledge in the form of stochastic constraints on the line parameters very effectively. The aesthetically pleasing model is transparent and accommodates various forms of control information, for example, full and partial control lines, parallel lines, with or without known distance.
- The collinearity approach is in essence an (image) point to a 3D line relationship. In contrast to the coplanarity approach, it does not require straight lines in the images. If used for every edge pixel, the proposed approach can be seen as a simultaneous combination of line fitting with orientation.

Line-based aerial triangulation will foster new applications. An increasing number of mapping projects are being carried out over areas with existing information, for example, for the purpose of map revision. Existing GIS information may furnish abundant control information, and the proposed method with its capability to stochastically model and analyze lines offers the potential to register new imagery to existing GIS data bases in an optimal fashion. Another interesting aspect of feature-based aerial triangulation is the combination with surface reconstruction. The tie lines are potential candidates for breaklines. Theoretically, a surface is reconstructed if all its breaklines (discontinuities in the surface function) are known because between breaklines, surface elevations can be predicted.

Realizing that we are just at the beginning of a truly feature-based aerial triangulation, it is no surprise that much more needs to be done. A major area of concern is the matching of linear features. Although numerous researchers have proposed feature-based matching methods, the problem of finding correspondences in multiple images has hardly been addressed. To come up with good initial estimates of the parameters in a highly nonlinear problem, such as aerial triangulation, is another concern.

Acknowledgements

Part of the research reported in this paper has been conducted during my sabbatical leave from OSU as a guest professor at the University of Applied Sciences in Stuttgart. Special thanks go to M. Hahn and colleagues for providing me with a ‘‘sanctuary’’ and for many stimulating discussions. I am also grateful to Garry Zalmanson, Technion, Israel. He did not only endure many nagging questions but offered great insight into the world of feature-based sensor orientation. Finally, I wish to thank the anonymous reviewers for their thoughtful recommendations to improve the quality of the paper.

References

Ayache, N., Faugeras, O., 1989. Maintaining representation of the environment of a mobile robot. IEEE Transactions on Robotics and Automation 5 (6), 804–819.

Ebner, H., Strunz, G., 1988. Combined point determination using digital terrain models as control information. International Archives of Photogrammetry and Remote Sensing 27 (B11/3), 578–587.

Förstner, W., 2000. New orientation procedures. International Archives of Photogrammetry, Remote Sensing and Spatial Information Sciences 33 (3), 297–304.

Habib, A., 1999. Areal triangulation using point and linear features. International Archives of Photogrammetry and Remote Sensing 32 (Part 3-2W5), 137–141.

Habib, A., Shin, S.W., Morgan, M., 2002. Automatic pose estimation of imagery using free-form control linear features. International Archives of Photogrammetry, Remote Sensing and Spatial Information Sciences 34 (Part 3A), 150–155.

Heikkilä, J., 1991. Use of linear features in digital photogrammetry. Photogrammetric Journal of Finland 12 (2), 40–56.

Heuvel, F., 2003. Automation in Architectural Photogrammetry. PhD thesis. Publications on Geodesy 54, NCG, Netherlands Geodetic Commission, Delft. 90 pp.

Jaw, J.J., 1999. Control Surface in Aerial Triangulation. PhD dissertation. Department of Civil and Environmental Engineering and Geodetic Science, The Ohio State University, Columbus, OH 43210. 98 pp.

Kubik, K., 1992. Photogrammetric restitution based on linear features. International Archives of Photogrammetry and Remote Sensing 29 (Part B3), 687–690.

Läbe, T., Henze, M., 2002. Automatische äussere Orientierung in der Orthophotoproduktion–ein Erfahrungsbericht. Proceedings of DGPF Conference, Band 11, Neubrandenburg, Germany, 24–26 September, 2002, DGPF Deutsche Gesellschaft für Photogrammetrie und Fernerkundung E.V., Berlin, pp. 245–252.

Lugnani, J.B., 1980. Using Digital Entities as Control. PhD thesis. Department of Surveying Engineering. University of New Brunswick, Fredericton. 159 pp.

Masry, S.E., 1981. Digital mapping using entities: a new concept. Photogrammetric Engineering and Remote Sensing 48 (11), 1561–1565.

Mikhail, E., 1993. Linear features for photogrammetric restitution and object completion. Proc. SPIE Conf. Integrating Photogrammetric Techniques with Scene Analysis and Machine Vision, vol. 1944, SPIE The International Society for Optical Engineering, Bellingham, WA, USA, pp. 16–30.

Mulawa, D.C., Mikhail, E.M., 1988. Photogrammetric treatment of linear features. International Archives of Photogrammetry and Remote Sensing 27 (Part B3), 383–393.

Patias, P., Petsa, E., Streilein, A., 1995. Digital Line Photogrammetry. Institute of Geodesy and Photogrammetry, Report 252, ETH Zürich. 54 pp.

Roberts, K.S., 1988. A new representation for lines. IEEE Proceedings of Computer Vision and Pattern Recognition, 635–640.

Schenk, T., 2002. Towards a Feature-Based Photogrammetry. Bildteknik/Image Science, 2002 (1), Swedish Society for Photogrammetry and Remote Sensing, Stockholm, pp. 143–150.

Schenk, T., 2004. Digital Photogrammetry, vol. 2. TerraScience, 16218 Bailor Rd., Laurelville, OH 43135. 366 pp.

Tommaselli, A., Lugnani, J., 1988. An alternative mathematical model to collinearity equations using straight features. International Archives of Photogrammetry and Remote Sensing 27 (Part B3), 765–774.

Zalmanson, G., 2000. Hierarchical Recovery of Exterior Orientation from Parametric and Natural 3D Curves. PhD dissertation. Department of Civil and Environmental Engineering and Geodetic Science, The Ohio State University, Columbus, OH 43210. 121 pp.

Zielinski, H., 1993. Object Reconstruction with Digital Line Photogrammetry. Doctoral thesis. Photogrammetric reports, No. 61, Royal Institute of Technology, Stockholm, Sweden. 115 pp.